Adsorption and Desorption of HCl on Ice

Marcia J. Isakson and Greg O. Sitz*

Department of Physics, University of Texas, Austin, Texas 78712

Received: October 21, 1998; In Final Form: January 25, 1999

Pulsed molecular beam and mass spectrometric techniques are used to study the adsorption of hydrogen chloride on thin ice films at temperatures from 100 to 170 K. The adsorption and desorption of HCl from an ice surface is relevant to the polar stratosphere where it is thought that chlorine atoms are liberated from reservoir species such as HCl by heterogeneous reactions occurring on the surface of polar stratospheric clouds. We have measured the sticking coefficient for HCl at an incident translational energy of 0.09 eV on thin film ice surfaces using a modified version of the reflectivity technique of King and Wells. By modeling the HCl partial pressure versus time waveforms for surface temperatures of 100−125 K, we obtain a sticking coefficient of 0.91 ± 0.06. The model incorporates first-order HCl desorption and a loss term also first order in HCl. Fitted kinetic parameters are $E_{des} = 28$ kJ/mol, $\nu_{des} = 2 \times 10^{14}$ s^{-1} for desorption and $E_{loss} = 21$ kJ/mol, $\nu_{loss} = 4 \times 10^{11}$ s^{-1} for the loss. The loss may be associated with the onset of water diffusion on the ice surface and subsequent ionization or hydration of the HCl. The measured waveforms are inconsistent with diffusion of HCl into the bulk. The apparent reflectivity decreases substantially in the temperature range of 126 to 140 K. This decrease cannot be attributed to an increase in sticking coefficient, a phase change in the ice, or the formation of the hexahydrate state of HCl.

1. Introduction

The seasonal depletion of ozone over the Antarctic (and very recently possibly over the Arctic) has been the subject of a great deal of attention in the past decade.[1,2] Although the depletion of ozone was reported by Farman et al. more than 10 years ago, the importance of heterogeneous processes has only recently begun to be appreciated.[1,3] It is now generally accepted that chemical reactions occurring on the surface of ice particles in polar stratospheric clouds (PSC's) play a crucial role in the catalytic cycle of chlorine responsible for the ozone destruction.[4,5] Ice particles in polar stratospheric clouds are believed to grow on sulfate aerosols and to form in two kinds: pure water ice and nitric acid trihydrate (NAT) ice.[6] The NAT ice particles (type I PSC's) are significant because they form at temperatures 5−7 K above that at which the pure ice crystals form, appearing earlier in the winter. The amount of nitric acid tied up in type I PSC's is also an important question since the removal of "odd nitrogen" (NO_2 and NO) from the gas phase affects the rates of other gas-phase reactions involving chlorine-containing species.[6]

A connection between the development of the seasonal ozone hole and the disappearance of the winter PSC's in the spring was reported by Hamill et al.[7] and Toon et al.,[8] and a mechanism involving the reaction

$$HCl + ClONO_2 \rightarrow Cl_2 + HNO_3 \qquad (1)$$

occurring on the ice surfaces was first proposed by Solomon et al.[4] The diatomic chlorine product is rapidly released into the atmosphere where it is quickly photolyzed into atomic chlorine (when the sunlight returns in the spring), which in turn, reacts readily with ozone:

$$Cl + O_3 \rightarrow ClO + O_2 \qquad (2)$$

Subsequent reactions involving the chlorine monoxide species regenerate a chlorine atom with the net result being loss of ozone in a catalytic cycle involving chlorine. Other relevant reactions produce the "reservoir" species HCl and $ClONO_2$, so-called because they contain chlorine in a relatively stable unreactive species.

Several groups have reported results from experiments using flow tube reactors that are relevant to these processes.[9−12] These groups measured the end products resulting from a given exposure of a chlorine-containing species to the inside of an ice coated tube at temperatures between 191 and 211 K. Results in the form of integrated reaction probabilities are obtained, but their methods are limited to reaction probabilities less than about 0.3[11] and do not address the elementary steps of adsorption/desorption rates and residence times. Leu[13] has reported similar flow tube measurements aimed at measuring sticking coefficients of HCl and other species, reporting a value for HCl of 0.4 (+0.6, −0.2). In the present work, we are able to obtain a considerably more accurate value for this number.

Graham and Roberts have studied the interaction of HCl with thin (1−20 ML) ice films grown on a W(100) substrate at 120 K using thermal programmed desorption.[14] They observe saturation of the bulk of the film at high HCl exposure and a molecular adsorbed HCl species when the bulk was saturated. The increase in the saturation yield with ice film thickness implies that HCl migration into the film is rapid at 120 K.

The importance of reaction 1 seems to be generally accepted even if the overall rate is only known approximately. However, theoretical work[15,16] concludes that the surface coverage of HCl on type II (pure) ice surfaces should be much too low for reaction 1 to occur at any appreciable rate. Theoretical work has also been reported on this system by Bussolin et al.[17] and

* Corresponding author. Phone: 1-512-471-0701. Fax: 1-512-471-9637. E-mail: gositz@physics.utexas.edu.

10.1021/jp984106g CCC: $18.00
Published on Web 03/11/1999

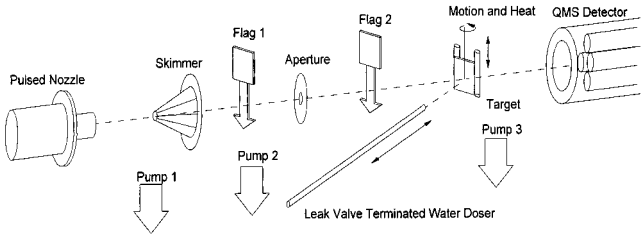

Figure 1. Schematic of the experimental setup. HCl molecules exit a supersonic molecule pulsed nozzle and pass through a skimmer into a differentially pumped buffer chamber. The molecules then pass through an aperture and are scattered from an ice film grown on a tantalum foil sample in a third chamber. Molecules are detected by a mass spectrometer. The water film is grown with a doser consisting of a quarter inch stainless steel tube terminated in a leak valve. Molecules can be blocked by quartz stops in the buffer and target chambers.

Gertner and Hynes.[18] Bussolini et al. calculate an energy for physisorption (and, through detailed balance, desorption) of 33.5 kJ/mol on the basal surface of ice using periodic two-dimensional calculations, molecular cluster calculations, and embedded cluster calculations. Kroes and Clary calculate an activation energy for desorption of 22−29 kJ/mol and a sticking coefficient of unity. Both of these values for desorption activation energy give a residence time at polar stratospheric temperatures of roughly 1 μs, which is much too short for a reaction with $ClONO_2$, even if the sticking coefficient (for $ClONO_2$) is unity. Gertner and Hynes propose an additional channel (other than desorption) whereby the HCl molecule is incorporated into the ice lattice in a stepwise ionization process. The activation energy for the first step in the process is 24−28 kJ/mol according to their model. Since the values for the activation energy of the first step of ionization and desorption are close, these processes will compete with each other, allowing a channel for HCl to remain on the surface and not desorb. Gertner and Hynes calculate that 40% of the HCl will desorb while 60% will be incorporated into the lattice at a temperature of 190 K.[18]

Here we report a measurement of the sticking coefficient for HCl on an ice surface. We also determine kinetic parameters for subsequent processes involving the adsorbed HCl. We use a different experimental approach than has been traditionally applied to laboratory studies of atmospheric processes. The technique is a modification of the molecular beam reflectivity method developed by King and Wells[19] that has been used extensively in measurements of sticking on metals and semiconductors. The extension described here utilizes a pulsed molecular beam; this allows for study of time-dependent phenomena such as desorption or diffusion following the initial adsorption of the gas on the surface. An existing alternative is the use of modulated molecular beams;[20] however, this is limited to relatively fast phenomena since the modulation frequency is typically 100−400 Hz.

2. Experimental Section

A schematic drawing of the apparatus is shown in Figure 1. It consisted of three differentially pumped chambers (the source, buffer, and target chambers) separated by two apertures. All three chambers were pumped by oil diffusion pumps; on the target chamber, the pump has a water cooled baffle. The base pressures in the three chambers were: source, 2×10^{-7} Torr; buffer, 8×10^{-8} Torr; target, 2×10^{-9} Torr.

The 25 L source chamber contains a pulsed, supersonic molecular beam (General Valve Series 9). This source was mounted on a flange that provides translation in three dimensions for accurate alignment. This source produced a pulse of 500 μs duration at a repetition rate of 0.6 Hz. The repetition rate was chosen to allow ample time for one pulse to be fully pumped away before the next pulse was fired. In the source chamber was a liquid nitrogen cooled surface to provide additional pumping speed for HCl. The stagnation pressure for the nozzle source was 28 psig. The beam exited the source chamber through a 0.5 mm diameter skimmer (Beam Dynamics, Inc.) into a buffer chamber. It was further collimated by a 2 mm aperture at the exit of the buffer chamber before entering the target chamber.

The molecular beam was pure HCl and had an energy of 90 meV, considerably higher than PSC kinetic energies of around 33 meV. Although the sticking coefficient at this incident energy may be lower than at energies relevant to PSC conditions, we did not decrease the incident energy (by seeding or other methods) because the experimental value for sticking coefficient we measured was already already close to unity.

The target chamber contained the sample manipulator. This consisted of a tantalum foil or graphite target clamped to two copper posts. The posts were part of a 1.33 in. conflat feedthrough which capped a liquid nitrogen reservoir. The copper thus provided rapid coupling to a heat sink. The sample was heated by passing current directly through it via the copper posts. The sample temperature was measured by means of a chromel−alumel thermocouple in direct contact with the front surface. The entire manipulator assembly was mounted on a stage that provided three orthogonal translational adjustments and rotation about a vertical axis.

Quartz beam stops could be inserted into the molecular beam independently in any of the three chambers. This was done to subtract off any HCl signal that reaches the target chamber resulting from effusion from the source or buffer chambers.

The target chamber was equipped with a quadrupole mass spectrometer (Vacuum Generators SX200) for measuring partial pressures. This instrument was located on the beam axis for optimization of the nozzle position before the target was lowered into the beam. The mass filter was set to mass 36 for measurements of HCl and mass 18 for the measurements of H_2O.

The target chamber also contained a doser for admitting water vapor to grow the ice films. This doser consisted of a quarter inch diameter stainless steel tube terminated in a leak valve. The tube/valve were mounted on a linear translation stage and could be moved close (<0.5 cm) to the sample so that the dose could be delivered directly to the graphite or tantalum target with a minimum of water escaping to the rest of the vacuum chamber. Distilled water was used that was further purified by several freeze/pump/thaw cycles. Film thickness was not well determined. We observed optical interference visually, so the thickness was greater than one-quarter of a visible wavelength. This implied that the layer was several thousand or more angstroms thick.

For waveform measurements, the partial pressure of HCl or DCl was monitored as a function of time preceding and following firing of the nozzle. Typically, the signal was recorded at a sampling rate of 500 Hz for about 1 s. Peak pressure rises were typically in the 10^{-12} mbar range.

Thermal programmed desorption was carried out by monitoring the partial pressure of HCl or DCl and ramping the temperature at a rate of approximately 10 K/s.

3. Results and Discussion

3.1. Temporal Waveforms. Measurements consisted of three parts: acquisition of reference, signal, and effusive (background)

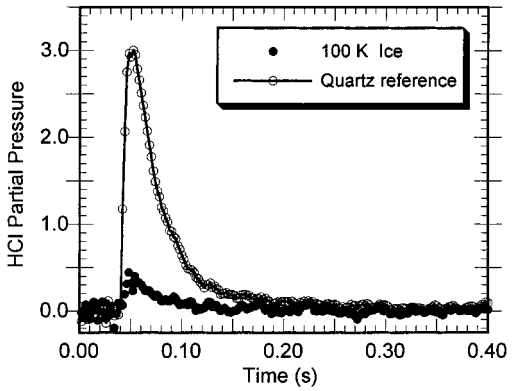

Figure 2. Reflectivity waveform data for HCl impinging on the main chamber quartz flag and on an ice film at 100 K. The difference in the peak height relates directly to the sticking coefficient.

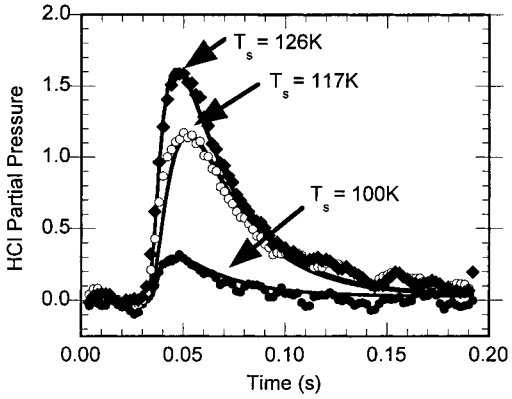

Figure 3. Waveform data as a function of ice film temperature (points) and fits to a model (described in the text). All three data sets plus one additional set at a temperature of 107 K (not shown for clarity) were simultaneously fit to obtain one set of parameters.

waveforms. The reference waveform was acquired by blocking the beam with the target chamber quartz flag. This flag was interposed in the beam just in front of the target and blocked the entire beam. The signal waveform was acquired with this flag moved out of the way, thus allowing the beam to strike the ice film. An additional waveform was measured by blocking the beam in the buffer chamber. This yielded the effusive background that was subtracted from the signal and reference waveforms prior to further analysis. The integrated effusive background was typically 25% of the reference signal.

Data taken according to this prescription are shown in Figure 2 for an ice temperature of 100 K. These data represent the average of 200 nozzle pulses. We saw no significant change in signal during one 200 pulse run, indicating that this dose is not saturating the surface. Data were taken for a range of ice temperatures. Results are shown in Figure 3 for ice temperatures from 100 to 126 K, along with results from a model discussed below. All the waveform data shown in Figures 2−4 have the effusive background subtracted off.

A calibration of the absolute beam dose supplied to the ice surface was problematic since it involved assumptions about the ice morphology, the beam profile, the absolute sensitivity of the mass spectrometer, and the pumping speed of the chamber, as well as others factors. Our best estimate of the beam dose is roughly 8×10^{11} molecules per cm^2 per pulse (0.001ML/pulse).

The waveform measurements were analyzed using a model to determine the sticking coefficient and kinetic parameters related to subsequent processes involving the HCl (detailed

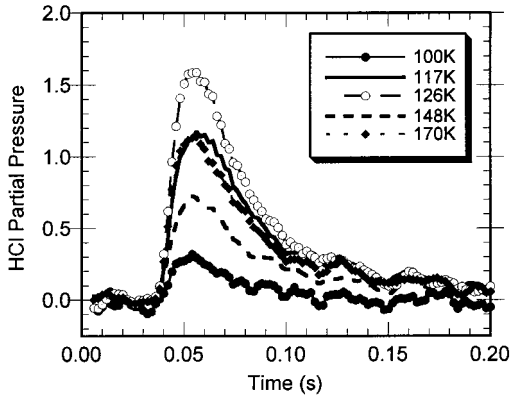

Figure 4. Waveforms taken at different ice temperatures. The apparent reflectivity initially increases as a result of an increase in the desorption rate, then falls dramatically between 126 and 140 K.

below). The modeling consisted of two parts. First, the reference waveform (with the effusive component subtracted) was modeled to determine the following system response parameters: pulse amplitude, pulse peak time, filling time constant, effective pumping speed, a sticking coefficient on background surfaces, and desorption from these background surfaces. Although this is a considerable number of parameters, each is related to a particular feature of the data. The amplitude corresponded to the integrated gas dose into the chamber; the time peak which corresponded to the center in time of the Gaussian pulse accounted for the onset; the filling time constant described the rise time of the pressure; the pumping speed accounts for the exponential pressure decay; the sticking and desorption on background surfaces was needed to describe the long-time tail of the curve which does not follow simple exponential decay. The parameters were used in a finite difference model to simulate HCl gas-phase density as a function of time, which was then compared to the pressure versus time recorded with the mass spectrometer. The parameters were adjusted to minimize the χ^2 of the residuals by Powell's direction set method.[21]

The parameters derived from the reference waveform model were fixed and used as input in a model for the data taken off the ice surface by incorporating additional physical processes relevant to the HCl/ice interaction. We modeled the data using sticking, desorption, and a first-order loss. By loss, we mean a process which makes the HCl unavailable for desorption. The results are shown in Figure 3 as solid lines. We emphasize that four data sets were simultaneously fit (only three are shown for clarity) to one set of parmeters: $S = 0.91 \pm 0.06$, $E_{des} = 28 \pm 2$ kJ/mol, $\nu_{des} = 2 \times 10^{14}$, $E_{loss} = 21 \pm 2$ kJ/mol, and $\nu_{loss} = 4 \times 10^{11}$ Hz. Note, a single (temperature independent) sticking coefficient was used to fit all the data in this temperature range. The activation energies are well determined from the fitting procedure as a result of having data sets for a range of temperatures. The preexponential factors are not determined as well. Based on fitting data sets from multiple days and on fits where one parameter is fixed and the remainder refit, we estimate that the preexponential factors are accurate to roughly a factor of 10.

There are some discrepancies between the data and the model shown in Figure 3. Small ice temperature variations (both absolute and gradients) are most likely responsible. For example, there are only 9 degrees difference between 126 and 117 K, the two top temperatures modeled. A half degree of change in temperature of both sets would change the difference in the desorption rates by 11%, which is significant in the model. Also,

the ice film which was about 5 mm in diameter and may have had a slight temperature variation across it.

The desorption parameters compare favorably to the values of $E_{des} = 33 \pm 5$ kJ/mol and $\nu_{des} = 1.0 \times 10^{13}$ Hz (assumed) determined by Graham and Roberts from thermal programmed desorption measurements.[14] However, the interpretation and application of these numbers requires some care; if only simple adsorption/desorption were occurring, then the HCl residence time would be 100 ms at 126 K and 5 μs at PSC temperatures of 190 K. Thus, without some other process, no significant HCl would be present at PSC temperatures. This is essentially the conclusion of Kroes and Clary.[15,16] Kroes and Clary had no other state available to bind the HCl more strongly in their calculation.

It is interesting to note that the activation energy for the loss channel in our kinetic model is very close to the activation energy for the first step in the stepwise ionization calculated by Gertner and Hynes.[18] Furthermore, it is also quite close to the value calculated for diffusion of water on an ice surface.[22] We speculate that diffusion of the water itself may be coming into play and that the water may then ionize or hydrate the HCl. Thus, some HCl molecules may be incorporated into the ice lattice and therefore no longer available for desorption.

Although the sticking coefficient determined from our model is high, it is not unity. We found that the tantalum foil used as a substrate was significantly more reflective to HCl (lower sticking coefficient and a lower activation energy for desorption) than was the ice film. However, since the HCl beam was significantly smaller than the ice film, we were able to use the difference in reflectivity between the tantalum foil and the ice film to position the molecular beam in the center of the ice film. Therefore, it is unlikely that the directly scattered HCl molecules are from the tantalum foil. It is also unlikely that they are from the effusive signal since we overestimate that signal by blocking it in the buffer chamber and not subtracting out the additional molecules that would have been directed into the main chamber. Since we never observed the directly scattered signal to completely disappear when exposed to ice (even at 98 K, the lowest temperature we could reach), we conclude that, at 0.09 eV incident energy, the sticking coefficient is less than unity.

It is known that the morphology of amorphous solid water (ASW) changes irreversibly with time at a rate that depends on deposition conditions.[23] This change is associated with a collapse of pores in the film. For our conditions, the time needed for this conversion is 10−100 times the time needed to acquire a waveform of the type shown in Figure 3. Thus, it seems unlikely that changes in ice morphology are responsible for the variation with temperature that we observe.

We have performed similar waveform measurements and analysis of crystalline ice in this temperature range. The thermal conversion of amorphous ice to the crystalline phase was followed by observing the drop in desorption rate as described by Smith et al.[24] The parameters determined were not significantly different from those obtained for scattering from the amorphous or unannealed ice. They were $S = 0.90$, $E_{des} = 26$ kJ/mol, $\nu_{des} = 1 \times 10^{13}$ Hz, E_{loss}, 24 kJ/mol, and $\nu_{loss} = 4 \times 10^{11}$ Hz.

3.2. Other Models. We tried unsuccessfully to model the data by incorporating processes other than a first order loss. Other processes considered were no diffusion or loss, (reversible) diffusion, and second-order desorption or loss. First, without some diffusion or loss channel the modeled waveforms indicated much more desorbing HCl than was observed and the data could not be fit with a consistent set of parameters. That is, if the surface temperature were high enough for any desorption, then eventually all the HCl would desorb; this was not observed experimentally. Second, we found that diffusion according to Fick's Law did not fit the data either. The reason for this is that if diffusion were fast enough to compete with desorption, then the HCl would diffuse back to the surface and desorb on the time scale of the experiment. This would lead to an increase in signal at longer times after the pulse, as well as a lack of HCl in postexposure TPDs (described below), neither of which was observed. This conclusion is in agreement with published results which show[25,10,11] that diffusion of HCl in ice is slow. Finally, a model with second-order diffusion or loss gave results which did not fit the shape of the waveform data nor give the correct temperature dependence.

3.3. Higher Temperatures. Waveform data was recorded at temperatures up to 170 K. Up to 126 K, the HCl signal rises which we interpret as adsorption with high probability followed by desorption in competition with a loss process as described above. Above 126 K, the peak amplitude of the waveforms decrease relative to that at 126 K as shown in Figure 4. We are unable to account for this observation within our model. However, we can exclude several factors from contributing to it. It is unlikely that the decrease in reflectivity is due to an increase in sticking coefficient, formation of the hexahydrate state, or a change in the ice morphology.

We can exclude an increase in sticking coefficient for two reasons. One, at ice temperatures of 100−126 K, the data are well described by a model with a (temperature independent) sticking coefficient of 0.91 ± 0.06. An increase in the sticking coefficient to unity would not alter the waveforms significantly given the desorption rate. Also, work done on nitrogen interaction with metal surfaces has shown that surface temperature does not significantly influence the sticking (or trapping) coefficient.[26]

Next, we can exclude the formation of the hexahydrate state as found by Banham et al.[27] They observed that this state forms around 165 K, a temperature much above that where we observe the reflectivity decrease. In addition, the phase diagram for HCl/ice as given by Molina[28] predicts the formation of this state at a higher temperature than our reflectivity decrease is observed.

Finally, we do not associate the drop in reflectivity with the crystallization of the ice film since we observed this same effect both in amorphous and crystalline (annealed) ice films.

3.4. Thermal Programmed Desorption. Thermal programmed desorption measurements were made for HCl exposures for ice temperatures in the range 100−170 K. The temperature in our experiment is limited by the onset of desorption of the ice itself. Results are shown in Figure 5 for HCl desorption following exposure at an ice temperature of 100 K. Similar measurements have been reported by Graham and Roberts[14] and Banham et al.[27] Unlike these groups, we did not observe a double peaked desorption signal. Based on the Redhead equation and the relevant heating rates, our observed TPD peak position is consistent with the second peak reported be Banham et al.[27] The lack of a low-temperature feature is most likely a result of the low exposure of HCl to the ice surface in our experiments. We found that the TPD yield for low-temperature exposure increased with an increasing number of beam pulses up to 500 pulses consistent with the loss mechanism in our model. We also found that the total TPD yield was complementary to the reflectivity; this is shown in Figure 6. The reflectivity was calculated by dividing the integral of the waveforms off the ice by the integral of the waveform off the

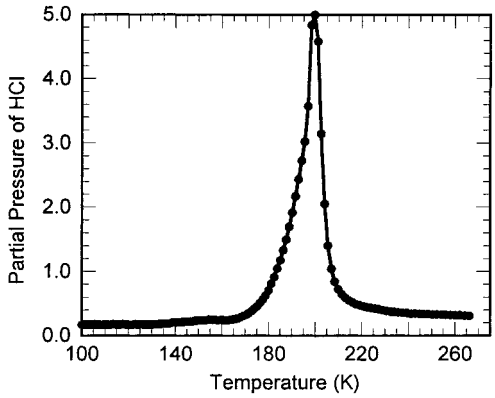

Figure 5. Typical thermal programmed desorption curve for HCl for adsorption at an ice temperature of 100 K. The heating rate was approximately 10 K/s. The double peaked structure seen in previous experiments[14] is absent because of low HCl exposure.

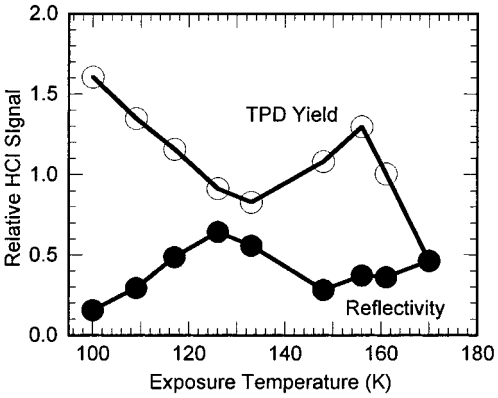

Figure 6. Reflectivity (integrated waveform from ice divided by integrated quartz flag waveform) and TPD yields for exposure at different ice film temperatures. The reflectivity and TPD yield are correlated except in the 170 and 159 K data in which the ice may be desorbing during the experiment. The correlation in the colder temperatures is consistent with the irreversible loss model.

quartz flag. Note that at the highest two temperatures, the TPD yield is lower than expected due to some desorption of the ice on the time scale of the experiment which apparently takes the HCl with it. These measurements show that the HCl is remaining on the ice for long times after exposure.

3.5. Implications for the Stratosphere. Based on the desorption activation energy measured by Graham and Roberts[14] and calculated by Kroes and Clary,[15,16] these groups concluded that HCl would not be available for reaction on polar stratospheric clouds due to the high desorption rate at PSC temperatures (180−205 K). However, the dramatic decrease in reflectivity above 126 K found in our experiments implies that the desorption parameters derived for HCl deposited at ice temperature less than 126−140 K as in Graham and Roberts' work are inapplicable for PSC temperatures, since other processes may be operative.

All our measurements are consistent with an initial sticking coefficient that is close to unity. A reasonable extrapolation suggests that the sticking coefficient at PSC temperatures is also high. Although we could not model the data at the higher temperatures (above 126 K), work on other substrates implies that surface temperatures should not significantly change the sticking coefficient. Furthermore, analysis limits the sticking coefficient to greater than 0.55 based solely on the total reflectivity. Last, we observe HCl in the TPD for exposures approaching PSC temperatures, implying the HCl is available for long times after exposure. This coupled with our finding that diffusion is not occurring at low temperatures implies that HCl is available near the ice surface for reaction at PSC temperatures.

The surface temperatures studied (100−170 K) are below the temperature of polar stratospheric clouds (180−205 K). As has been discussed by Brown and George,[29] ice surfaces at PSC temperatures are in dynamic equilibrium with 10−100 monolayers adsorbing and desorbing per second. The time scale of the present experiments precludes working under these conditions.

4. Conclusion

In conclusion, we have used the modified King and Wells technique and thermal programmed desorption to investigate the reaction of HCl with amorphous and crystalline ice. We conclude that the sticking coefficient of this system is 0.91 ± 0.06. We calculate the desorption activation energy for temperatures less than 126 K to be 28 ± 2 kJ/mol with a preexponential factor of 2×10^{14} Hz and an irreversible loss activation energy to be 21 ± 2 kJ/mol with a preexponential of 4×10^{11} Hz. A decrease in reflectivity for temperatures above 126 K was found in all waveform measurements. This decrease is not a result of an increase in the sticking coefficient, the formation of a hexahydrate state, or the crystallization of the ice film.

References and Notes

(1) See, for example, the entire issue D9, volume 94 of Journal of Geophysical Research, 1989. Some specific references from this issue are given below.

(2) Chemical kinetics and photochemical data for use in stratospheric modeling. JPL Publication 94-26, 1994.

(3) Farman, J. C.; Gardiner, B. C.; Shanklin, J. D. *Nature* **1985**, *315*, 207−210.

(4) Solomon, S.; Garcia, R. R.; Rowland, F. S.; Wuebbles, D. J. *Nature* **1986**, *321*, 755−758.

(5) Molina, M. J.; Tso, T. Y.; Molina, L. T.; Wang, F. C. Y. *Science* **1987**, *238*, 1253−1257.

(6) Fahey, D. W.; Kelly, K. K.; Ferry, G. V.; Poole, L. R.; Wilson, J. C.; Murphy, D. M.; Loewenstein, M.; Chan, K. R. *J. Geophys. Res.* **1989**, *94*, 11299−11315.

(7) Hamill, P. R.; Toon, O. B.; Turco, R. P. *Geophys. Res. Lett.* **1986**, *13*, 1288−1292.

(8) Toon, O. B.; Hamill, P.; Turco, R. P.; Pinto, J. *Geophys. Res. Lett.* **1986**, *13*, 1284−1287.

(9) Tolbert, M. A.; Rossi, M. J.; Malhotra, R.; Golden, D. M. *Science* **1987**, *238*, 1258−1260.

(10) Hanson, D. R.; Ravishankara, A. R. *J. Geophys. Res.* **1991**, *96*, 5081−5090.

(11) Hanson, D. R.; Ravishankara, A. R. *J. Phys. Chem.* **1992**, *96*, 2682−2691.

(12) Abbatt, J. P. D.; Molina, M. J. *J. Phys. Chem.* **1992**, *96*, 7674−7697.

(13) Leu, M. T. *Geophys. Res. Lett.* **1988**, *15* (1), 17−20.

(14) Graham, J. D.; Roberts, J. T. *J. Phys. Chem.* **1994**, *98*, 5974−5983.

(15) Kroes, G. J.; Clary, D. C. *Geophys. Res. Lett.* **1992**, *19*, 1355−1358.

(16) Kroes, G. J.; Clary, D. C. *J. Phys. Chem.* **1992**, *96*, 7079−7080.

(17) Bussolin, G.; Casassa, S.; Pisani, C.; Ugliengo, P. *J. Chem. Phys.* **1998**, *108*, 9516−9528.

(18) Gertner, B. J.; Hynes, J. T. *Science* **1996**, *271*, 1563−1566.

(19) King, D. A.; Wells, M. G. *Surf. Sci.* **1972**, *29*, 454−482.

(20) Padowitz, D. F.; Peterlinz, K. A.; Sibener, S. J. *Langmuir* **1991**, *7*, 2566−2576.

(21) Press, W. H.; Flannery, B. P.; Teukolsky, S. A.; Vetterling, W. T. *Numerical Recipes*; Cambridge University Press: Cambridge, MA, 1986; Chapter 10.

(22) Batista, E.; Jonsson, H. Private communication, 1998.

(23) Zondlo, M. A.; Onasch, T. B.; Warshawsky, M. S.; Tolbert, M. A.; Mallick G.; Arentz, P.; Robinson, M. S. *J. Phys. Chem. B* **1997**, *101*, 10887−10895.

(24) Smith, R. S.; Huang, C.; Wong, E. K. L.; Kay, B. D. *Surf. Sci.* **1996**, *367*, L13−L18.

(25) Wolff, E. W.; Mulvaney, R. *Geophys. Res. Lett.* **1989**, *16* (6), 487−490.
(26) Rettner, C. T.; Schweizer, E. K.; Stein, H.; Auerbach, D. J. *Phys. Res. Lett.* **1988**, *61*, 986−989.
(27) Banham, S. F.; Sodeau, J. R.; Horn, A. B.; McCoustra, M. R. S.; Chesters, M. A. *J. Vac. Sci. Technol. A* **1996**, *14* (3), 1620−1626.
(28) Molina, M. J. "The Probable Role of Stratospheric Ice Clouds: Heterogeneous Chemistry of the Ozone Hole." *The Chemistry of the Atmosphere: Its Impact on Global Change*; Calvert, J. G., Ed.; Blackwell Scientific: Boston, 1994, Chapter 3.
(29) Brown, D. E.; George, S. M. *J. Phys. Chem.* **1996**, *100* (38), 15460−15469.